Toxoplasma gondii myosin F, an essential motor for centrosomes positioning and apicoplast inheritance

Damien Jacot, Wassim Daher and Dominique Soldati-Favre

Supplementary information

Supplementary Materials and Methods

Antibodies

The antibodies used in this study are described as follows: rabbit polyclonal; α-CAT (Ding et al, 2000), α-GAP45 (Plattner et al, 2008), α-PfPRF (Plattner et al, 2008), α-Cpn60 (Agrawal et al, 2009), α-HSP70 (Pino et al, 2010), α-GFP (Clonetech, 632460); mouse monoclonal, α-ACT (Herm-Gotz et al, 2002), α-ATrx1 (DeRocher et al, 2008), α-ISP1 (Beck et al, 2010), α-SAG-1 (T4-1E5) (Frenal et al, 2010), α-MIC3 (T42F3) (El Hajj et al, 2008), α-Rop2-4 (T3-4A7) (Sadak et al, 1988), α-Ty (BB2), α-Myc (9E10), α-HA (16B12, Covance Inc). Mouse monoclonal antibodies α-5F4 (α-F1-ATPase beta subunit) and α-ROP7 (1B10) were a gift from Peter Bradley (University of California, USA). Rabbit polyclonal α-Centrin1 antibodies were kindly provided by Marc-Jan Gubbels (Boston College, MA, USA). Visualization of the Golgi was through transient transfection of pT8-GRASP-YFP (Pelletier et al, 2002). For Western blot analysis, secondary peroxidase conjugated goat α-rabbit and α-mouse Abs (Molecular Probes, Paisley, UK) were used. For immunofluorescence analysis, the secondary Abs Alexa Fluor 488-conjugated goat α-rabbit IgG Abs and Alexa Fluor 594-conjugated goat α-mouse Abs (Molecular Probes, Invitrogen) were used.

Cloning of DNA constructs

Genomic DNA was isolated with the Wizard SV genomic DNA purification system (Promega). RNA was isolated using Trizol (Invitrogen) extraction. The cDNA was generated by RT-PCR performed with the Superscript II reverse transcriptase (Invitrogen) according to the manufacturer's protocol. TgMyoF GenBank accession number: DQ131541.

TgMyoF-neck/tail fragment was amplified using primers 1375/3634 (Table S1) and TgMyoF-tail with primers 3634/3643 and cloned in pTub8DDmycFH2-HX (Daher et al, 2010) between *Nsi*I/*Pac*I. TgMyoF-WD40 fragment was amplified using primers 3634/3831 and cloned between *Nsi*I/*Pac*I in pT8DDMycHis-TgROM4mut-HX (Santos et al, 2011). For pT8DDmycGFPTgMyoF-tail-HX-ble, GFP was amplified using primers 455/880 with pT8mycGFP-PfMyoAtailTy-HX (Herm-Gotz et al, 2002) as template. PCR product was digested with *Nsi*I and cloned in pT8DDmycTgMyoF-tail-HX at the *Nsi*I site. Bleomycin resistane gene (ble) expressing cassette was digested with *Not*I from p3011-Ty-TgPRF-ble (Plattner et al, 2008) and cloned in pT8DDmycGFPTgMyoF-tail-HX at the *Not*I site. Genomic DNA from RH strain was used as a template for the following cloning. TgMyoF-3Ty was amplified with primers 2717/3633 and cloned in pT8-TgMIC13-3Ty-HX (Friedrich et al, 2010) between *Kpn*I and *Nsi*I sites. 5'MyoF-TATi1-HX-tetOpS1MycNtMyoF; the 5'MyoF fragment was amplified using primers 3660/3661 and cloned between *Nco*I and *Bam*HI in 5'COR-pT8TATi1-HX-tetOpS1MycNtCOR (Salamun et al, unpublished). NtMyoF was amplified with primers 3654/3655 and cloned between *Bgl*II and *Spe*I in the same plasmid. All fragments were sequenced prior to transfection.

Immunofluorescence assay (IFA) and confocal microscopy

HFFs seeded on cover slips in 24-well plates were inoculated with freshly released parasites. After 2-5 rounds of parasite replication, cells were fixed with 4% paraformaldehyde (PFA) or

4% PFA/0.05% glutaraldehyde (PFA/GA) in PBS, neutralized 3–5 min in 0.1 M glycine/PBS, and processed as previously described (Plattner et al, 2008). Confocal images were generated with a Leica laser scanning confocal microscope (TCS-NT DM/IRB and SP2) using a 100 x Plan-APO objective with NA 1.4.

Live microscopy

Freshly egressed DDMyoF-tail expressing parasites were transfected with 15-30 µg of pT8GAP45Ct-GFP (Frenal et al, 2010) or pT8TgACP-DsRed-Ty-HX (Pino et al, 2007), inoculated onto HFF monolayer coverslips and incubated for 14 h. Parasites were washed and treated ± Shld-1 for 4 h. HEPES was added to the culture at a final concentration of 10 mM for live microscopy recording. Stacks were taken every 10 min. Microscope: Nikon Eclipse TE2000-U, CSU 21 Yokogawa spinning disk head; Objectives: Nikon Plan Apo 100x/1.4 DIC H with Piezzo; Detector: Andor iXON EM +; image stacks were processed with ImageJ using maximum intensity Z projection.

Egress Assay

Freshly egressed parasites were allowed to invade HFF monolayers on coverslips and incubated for 2 h. A pre-treatment for 12 h (± ATc) was performed for TgMyoF-iKO. After 30 h of culture ± ATc or ± Shld-1, parasites were treated for 7 min at 37°C with DMEM containing 0.06% DMSO or 3 µM Ca2+ ionophore A23187 (from Streptomyces chartreusensis, Calbiochem 100105). The coverslips were fixed with PFA/GA and stained with anti-GAP45 antibodies. 200 vacuoles were counted for each strain and the number of egressed vacuoles is represented. Data are mean values ± SD from three independent biological experiments.

Invasion Assay Red/Green

Freshly egressed parasites treated ± ATc for 48 h or ± Shld-1 for 24 h were allowed to invade HFF monolayers on coverslips for 30 min before fixation with PFA/GA for 7 min. Fixed cells were blocked 30 min with 2% BSA/PBS, incubated with anti-SAG1 antibodies diluted in 2% BSA/PBS for 20 min and washed 3 times with PBS. Cells were then fixed with 1% formaldehyde/PBS for 7 min and washed once with PBS. Permeabilization using 0.2% Triton X-100/PBS was performed for 20 min. A second incubation using anti-GAP45 antibodies diluted in 2% BSA/0.2% Triton X-100/PBS was performed. Cells were then washed 3 times with 0.2% Triton X-100/PBS. Incubation with secondary antibodies was performed as described previously. 200 parasites were counted for each condition and the percentage of intracellular parasites is represented. Data are mean values ± SD from three independent biological experiments.

Co-immunoprecipitation

Intracellular parasites (30 h post infection) were harvested, washed in PBS and lysed in IP buffer (1% Triton X-100/PBS) in the presence of a protease inhibitor cocktail (Roche). Lysates were incubated for 10 min on ice and centrifuged at 14,000 rpm for 30 min. Supernatants were incubated with the GFP-Trap® (ChromoTek GmbH) for 1 h at 4°C on a wheel. The Complexes were then washed five times in the IP buffer. Finally, beads were re-suspended into SDS–PAGE loading buffer and boiled at 95°C for 5 min prior SDS-PAGE.

Western blot analysis

Parasites were lysed in RIPA buffer (150 mM NaCl, 1% Triton X-100, 0.5% deoxycholate, 0.1% SDS, 50 mM Tris pH 7.5) using standard procedures and mixed with SDS–PAGE loading buffer. Suspension was subjected to two sonication cycles. SDS-PAGE was

performed using standard methods. Separated proteins were transferred to nitrocellulose membranes and probed with appropriate antibodies in 5% non-fat milk powder in 1X PBS-0.05% Tween20. Bound secondary peroxidase conjugated antibodies were visualized using either the ECL system (Amersham Corp) or SuperSignal (Pierce).

Western blot quantification

The percentage of pCpn60 over the total amount of Cpn60 was quantified using Multi Gauge V3.0 following manufacturer's protocol. Data are mean values ± SD from three independent biological experiments.

Quantitative real time PCR (qRT-PCR)

MyoF-iKO parasites were treated 48 h ± ATc. RNA was extracted with GenElute Mammalian Total RNA Miniprep Kit (Sigma) according to manufacturer's protocol. SuperScript II Reverse Transcriptase (Invitrogen) was used for reverse transcription. qRT-PCR was performed using SYBR Green JumpStar *Taq* ReadyMix from Sigma. Primers qRT 1-2 were used to assess the regulation of *iMycMyoF*. Primers qRT 3-4 were used to compare the level of expression of *iMycMyoF* ± ATc compare to the endogenous *MyoF* in Ku80-KO. qRT-PCR results were normalized to tubulin beta chain (TGME49_266960) (primers qRT 5-6). Data are presented as mean value ± SD of three independent biological experiments.

Supplementary Table S1

Oligonucleotide primers used in this study; restriction sites are underlined and coding sequence are in uppercase.

Primer	Orientation	5'-3' sequence
455	reverse	ccaatgcatTTTGTATAGTTCATCCATGCCATGTG
880	sense	GGTGTTACACAATCACC
1375	sense	ccggcctgcaggGGAAGACCCTCTGCTTCTTC
C	sense	cgctgcaccacttcattatttcttctgg
2717	sense	ccgggtaccactgaacttctcctgaattcctttg
B	reverse	GAGCGAGTTTCCTTGTCGTCAGGCC
3633	reverse	gcgatgcatgGACAGCTCGACCTCGCGCCCCCCCG
3634	reverse	gcgttaattaaCTAGACAGCTCGACCTCGCGCC
3643	sense	gccatgcatGAGGAGGCTCGCGAGGTCTCAGGCCTTC
G	reverse	GTTGTCTGCTGTTTCGAGAGCGC
3654	sense	gcgggatccATGACGGCATCTTCTGCAGATGGG
3655	reverse	gcgactagtGAGACAAGAAACGACAGACGCATGC
3660/F	reverse	cgcggatcccaacgcagattgcacgcggcac
3661	sense	gcgccatggcctgcaggcagacgagaggtagcgaagcgc
D	reverse	cggcgcactcagtccggtggtg
3831	sense	gcgatgcatCTCTCACAGTCGTCGATGCGACCTG
3857	sense	gccatgcatATGAGAGAGGTTATCAGCATCCACGTC
3858	reverse	gcgttaattaaTTAGTACTCGTCACCATAGCCCTCCTC
A	sense	cagccgttgcctgaacaccggcg
E	sense	CATTTATCAGGGTTATTGTCTCATGAGCG
qRT1	sense	AGCAGAAGCTCATCTCCGAGGAGGACCTG
qRT2	reverse	AGCATCGTCAAATCTGTCGGCGCACTCAG
qRT3	sense	GGAGAGCGGAGCAGGCAAGACAGAAA
qRT4	reverse	TCGGGGAAGGGAAGTAATAGATGC
qRT5	sense	CGCCACGGCCGCTACCTGACT
qRT6	reverse	TACGCGCCTTCCTCTGCACCC

Supplementary figures

Figure S1. (A) Western blot analysis of parasites treated ± 0.3 µM CD from ring to trophozoite stage (12 h) or from trophozoite to schizont stage (12 h) using anti-GFP antibodies. The CD treatment did not affect the processing of PfSOD2-GFP. Detection of *P. falciparum* profilin was used as a loading control. pSOD2-GFP, SOD2-GFP precursor; mSOD2-GFP, SOD2-GFP mature. (B) Live microscopy of a *P. berghei* strain expressing PbACP-GFP protein treated 14 h ± 0.3 µM CD *in vitro*. The apicoplast failed to associate with the forming schizonts and accumulated in close proximity of the food vacuole. (C) All egressed merozoites contain an apicoplast in non-treated parasites. Scale bar 5 µm.

Figure S2. (A) Time course ATc treatment of TgPRF-iKO and TgPRF-iKO+WTC. After a short-term treatment (48 h ± ATc) the apicoplast was lost only in a few vacuoles. However, after a prolonged treatment, the majority of vacuoles are lacking this organelle. Data are mean values ± SD from three independent experiments where 200 vacuoles were counted for each condition. (B, C) Apicoplast inheritance was not affected 36 h after stabilization of DDFH2/1 or DDFH2/2-R/A. (D) Rhoptries were only slightly affected following 72 h depletion of TgPRF, 48 h depletion of ADF or 36 h stabilization of DDFH2/2. In some cases the organelles accumulated in enlarged residual bodies (arrow). Scale bar 2 µm.

Figure S3. (A) Down-regulation of MyoA-iKO detected with anti-Myc antibodies 48 h after ATc treatment. (B) Apicoplast inheritance is not affected following 48 h of MyoA depletion. (C) Apicomplexan MyoFs share a conserved architecture including variable numbers of WD40 and coiled-coil domains and putative IQ motifs. PfMyoF, PF3D7_1329100; PbMyoF, PBANKA_134410; TaMyoF, TA06960; BbMyoF, XP_001611026.1;

CpMyoF, EAK90169; GpMyoF, ABR21557.1. (D) Treatment of extracellular parasites for 15 min with 1 μM CD or 1 μM jasplakinolide (Jas) did not affect the localization of MyoF-3Ty. The motor accumulates on top of nucleus and is present throughout the cytoplasm and at the pellicle. (E) 15 min Jas treatment at 1 μM affects parasite's actin as previously described (Wetzel et al, 2003). Scale bar 2 μm.

Figure S4. (A) Schematic representation of MyoF-iKO recombinant locus (not to scale). A construct allowing the insertion of a cassette expressing the transactivator TATi-1 and the replacement of *TgMyoF* promoter with the 7-tet-Op Sag1 (TetO7) inducible promoter was introduced by double homologous recombination in *TgMyoF* locus. Additionally, a Myc tag was inserted at the N-terminus of TgMyoF. Upon addition of ATc, the gene is silenced. (B) PCR analysis of MyoF-iKO recombinant locus using primers presented in panel (A). The absence of integration in the 5' (AB 1756 bp) suggests that only a single homologous recombination event in the N-terminal of MyoF (primer CD 1165 bp) took place. As this integration is reversible, endogenous locus was weakly amplified (primers AD, 2866 bp). Only the primer AD gave a product with Ku80-KO genomic DNA. (C) Although the MyoF-iKO vector was linearized prior to electroporation, some molecules could still be circular and account for single homologous recombination events. In the MyoF-iKO clone investigated here, the vector integrated by single homologous recombination downstream of the ATG. The resulting locus still contains the backbone vector (primers EF, 1820 bp). Following such a recombination event the promoter of *MyoF* is displaced and the regions of *MyoF* locus used for recombination are duplicated (primers AG, 1880 bp). Further analysis of the modified genomic locus indicate that likely more than one copy of the plasmid have integrated on the 5'end. Multiple primer pairs were used to assess the topology of the 5' recombinant locus but due to overlapping sequences we were not able to resolve the exact configuration of the locus.

(D) We have generated an independent clone where double recombination occurred. Genomic PCR analysis of *MyoF-iKO* recombinant locus using primers A/B and C/D confirmed integration by double homologous recombination. The endogenous locus amplified with primers A/D is only present in the parental strain Ku80-KO. This new clone was investigated and shown to recapitulate all the phenotypes observed with the clone reported here (E) The left panel represents the relative transcript levels of *iMycMyoF* after 48 h ± ATc as determined by quantitative PCR with primers qRT 1-2. The right panel represents the relative levels of *iMycMyoF* after 48 ± ATc compare to the endogenous *MyoF* in Ku80-KO (primers qRTq 3-4). qRT-PCR results were normalized to parasite's tubulin beta chain. Data are presented as mean value ± SD of three independent biological experiments. (F) Egress assay of Ku80-KO and MyoF-iKO parasites treated for 42 h with ATc prior to calcium ionophore induction of egress. (G) Invasion assay of Ku80-KO and MyoF-iKO parasites treated for 48 h with ATc. MyoF depleted parasites were not affected in invasion. Data are mean values ± SD from three independent experiments where 200 vacuoles/parasites were counted for each condition. (H) Plaque assays on Ku80-KO and MyoF-iKO parasites after seven days of culture in presence or absence of ATc. Only parasite depleted in MyoF failed to form plaques.

Figure S5. (A) Shld-1 dependent stabilization of DDMyoF-WD40 (60 kDa) and DDMyoF-neck/tail (138 kDa) by Western blot using anti-Myc antibodies. *T. gondii* actin was used as a loading control. (B) IFA performed on parasites expressing DDMyoF-neck/tail (treated with Shld-1 for 24 h). The apicoplast is detected with anti-ATrx1 antibodies and the rhoptries with anti-ROP2-4. GAP45 staining showed severe defects at the pellicle (arrow). Scale bar 2 μm. (C) Intracellular growth analysis at 30 h revealed a block at 2-4 parasites per vacuoles in DDMyoF-neck/tail expressing parasites. Data are mean values ± SD from three independent experiments where 200 vacuoles were counted for each condition. (D) Parasites expressing

DDMyoF-WD40 were not affected in their lytic cycle after seven days. (E-F) DDMyoF-tail expressing parasites were not affected in invasion or egress after 48 h and 30 h Shld-1 treatment respectively. Data are mean values ± SD from three independent experiments where 200 vacuoles were counted for each condition. (G) Parasites expressing DDMyoF-tail failed to form plaques after seven days. RH and non-treated parasites formed plaques of comparable sizes. (H) Western blot analysis using anti-Myc antibodies showed the stabilization of DDGFPMyoF-tail at the predicted size (145 kDa) after a Shld-1 treatment of 36 h.

Figure S1

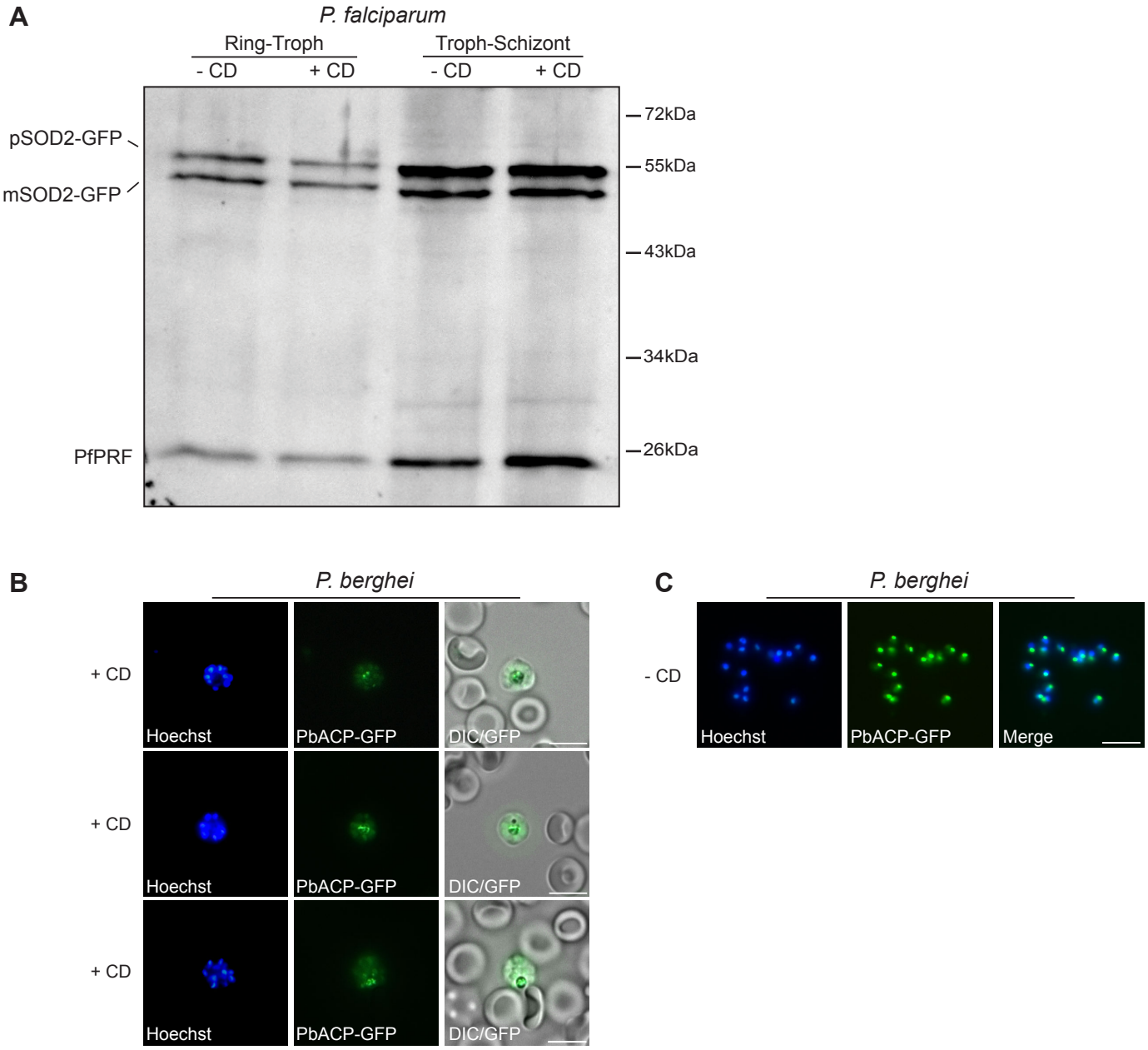
A
P. falciparum
Ring-Troph
Troph-Schizont
- CD
+ CD
- CD
+ CD
pSOD2-GFP
mSOD2-GFP
PfPRF
72kDa
55kDa
43kDa
34kDa
26kDa
B
P. berghei
+ CD
+ CD
+ CD
Hoechst
PbACP-GFP
DIC/GFP
C
P. berghei
- CD
Hoechst
PbACP-GFP
Merge

Figure S2

A

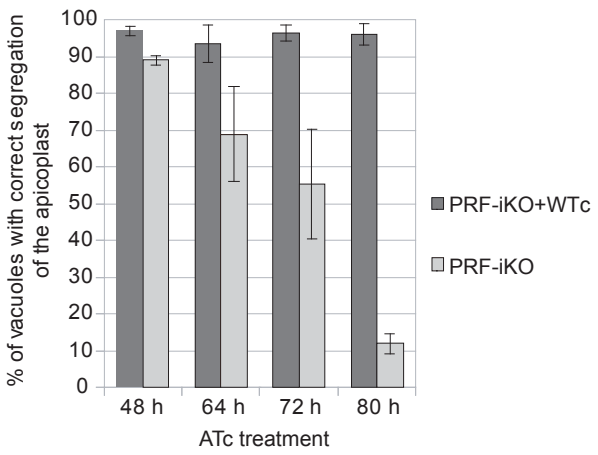

B

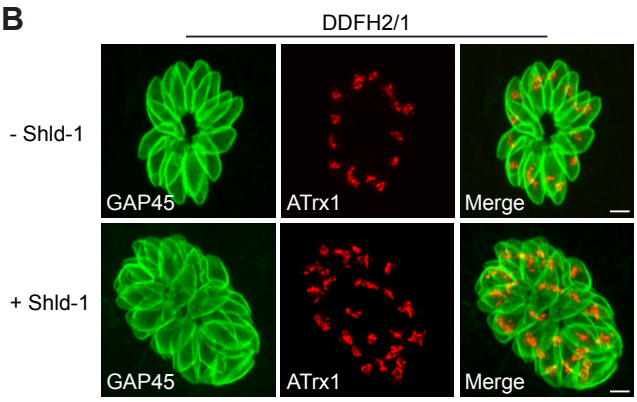

C

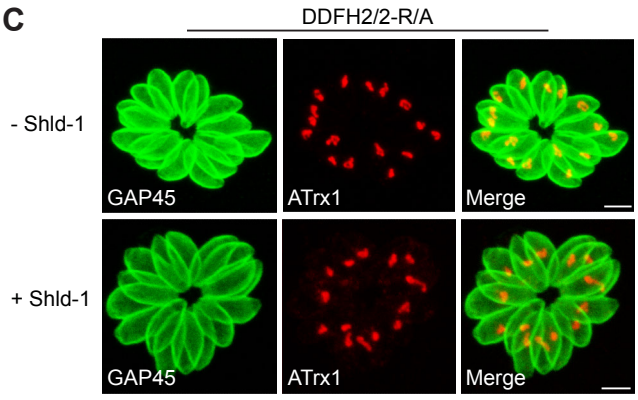

D

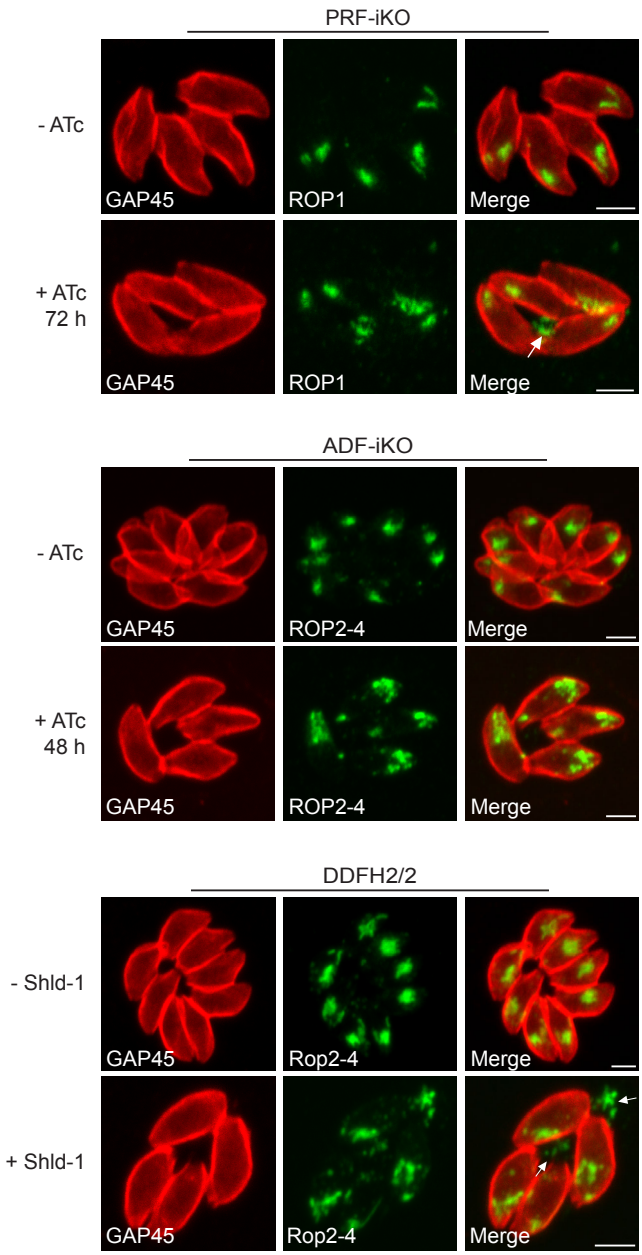

Figure S3

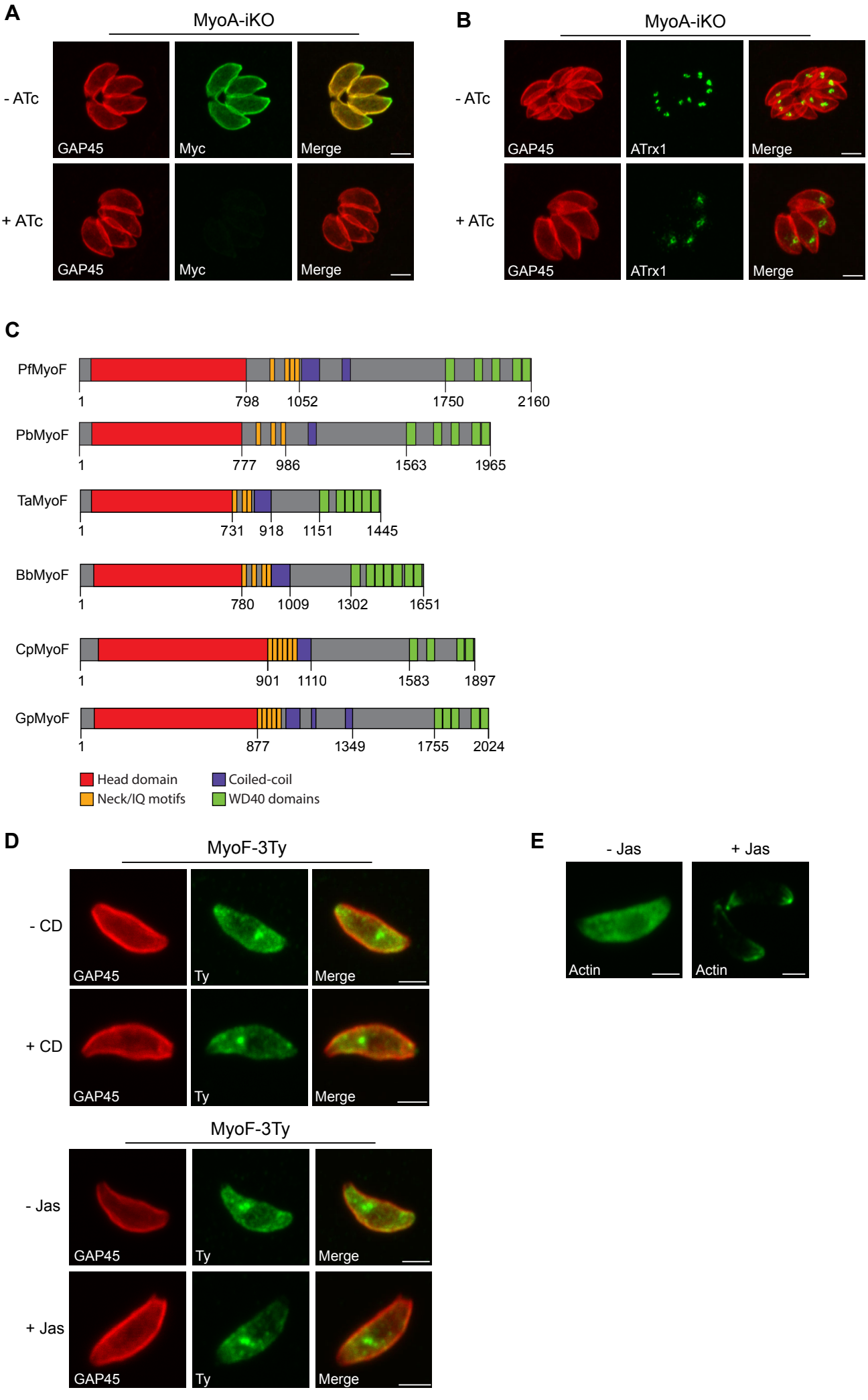
A
MyoA-iKO
- ATc
+ ATc
GAP45
Myc
Merge
B
MyoA-iKO
- ATc
+ ATc
GAP45
ATrx1
Merge
C
PfMyoF
1
798
1052
1750
2160
PbMyoF
1
777
986
1563
1965
TaMyoF
1
731
918
1151
1445
BbMyoF
1
780
1009
1302
1651
CpMyoF
1
901
1110
1583
1897
GpMyoF
1
877
1349
1755
2024
Head domain
Coiled-coil
Neck/IQ motifs
WD40 domains
D
MyoF-3Ty
- CD
+ CD
GAP45
Ty
Merge
MyoF-3Ty
- Jas
+ Jas
E
- Jas
+ Jas
Actin

Figure S4

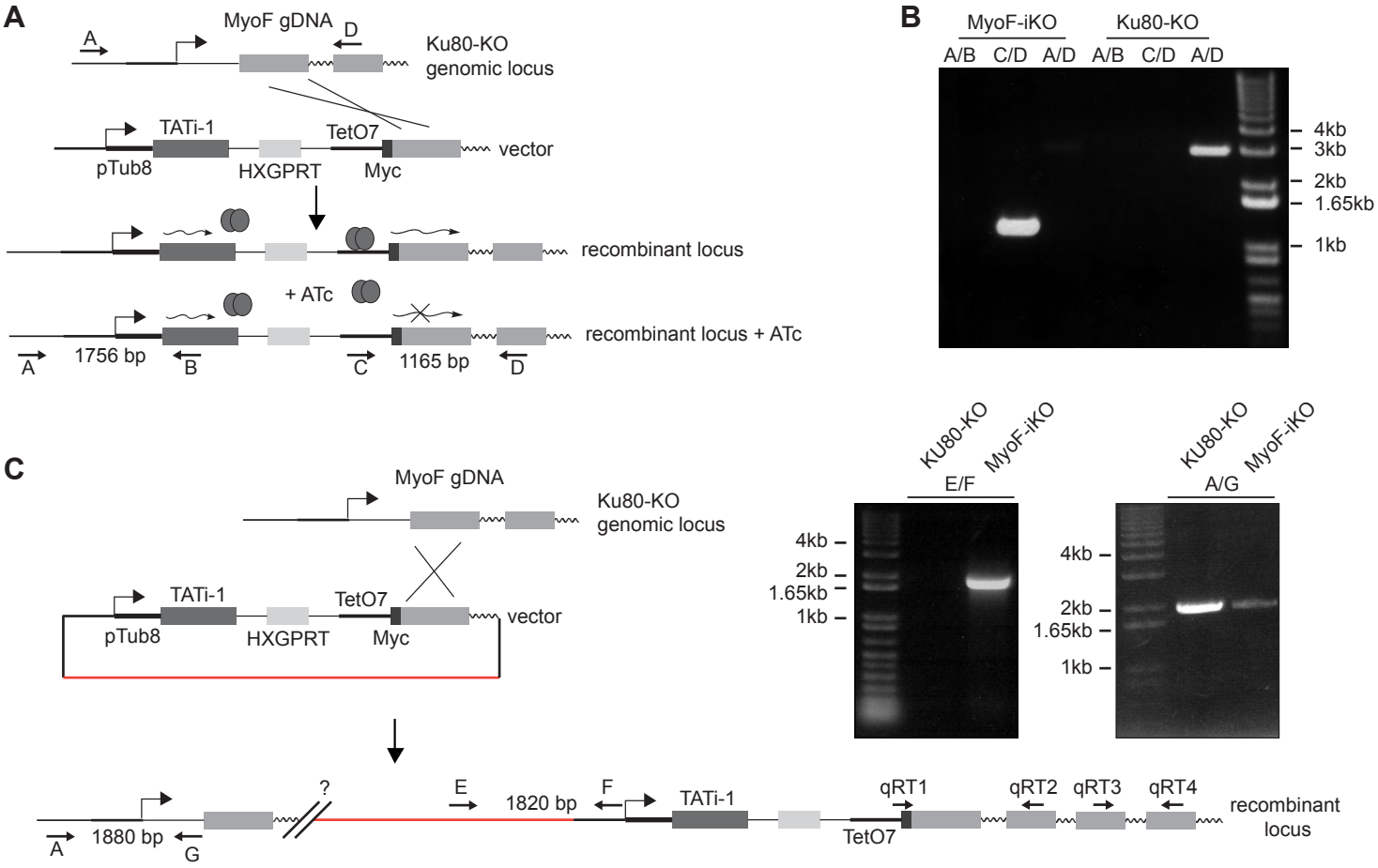
A
MyoF gDNA
A
D
Ku80-KO
genomic locus
TATi-1
TetO7
vector
pTub8
HXGPRT
Myc
recombinant locus
+ ATc
recombinant locus + ATc
1756 bp
1165 bp
B
MyoF-iKO
Ku80-KO
A/B C/D A/D A/B C/D A/D
4kb
3kb
2kb
1.65kb
1kb
C
MyoF gDNA
Ku80-KO
genomic locus
TATi-1
TetO7
vector
pTub8
HXGPRT
Myc
KU80-KO
MyoF-iKO
E/F
A/G
4kb
2kb
1.65kb
1kb
?
E
1820 bp
F
TATi-1
qRT1
qRT2
qRT3
qRT4
TetO7
recombinant
locus
1880 bp
G
D
MyoF-iKO
Ku80-KO
A/B C/D A/D A/B C/D A/D
4kb
3kb
2kb
1.65kb
1kb
E
qRT 1-2
Relative fold expression
MyoF-iKO
- ATc
+ ATc
qRT 3-4
Relative fold expression
MyoF-iKO
Ku80
Ku80
- ATc
+ ATc
F
% of egressed parasites
MyoF-iKO - ATc
MyoF-iKO + ATc
Ku80 - ATc
Ku80 + ATc
DMSO
A23187
G
% of invasion
- ATc
+ ATc
MyoF-iKO
Ku80
H
Ku80-KO
MyoF-iKO
- ATc
+ ATc

Figure S5

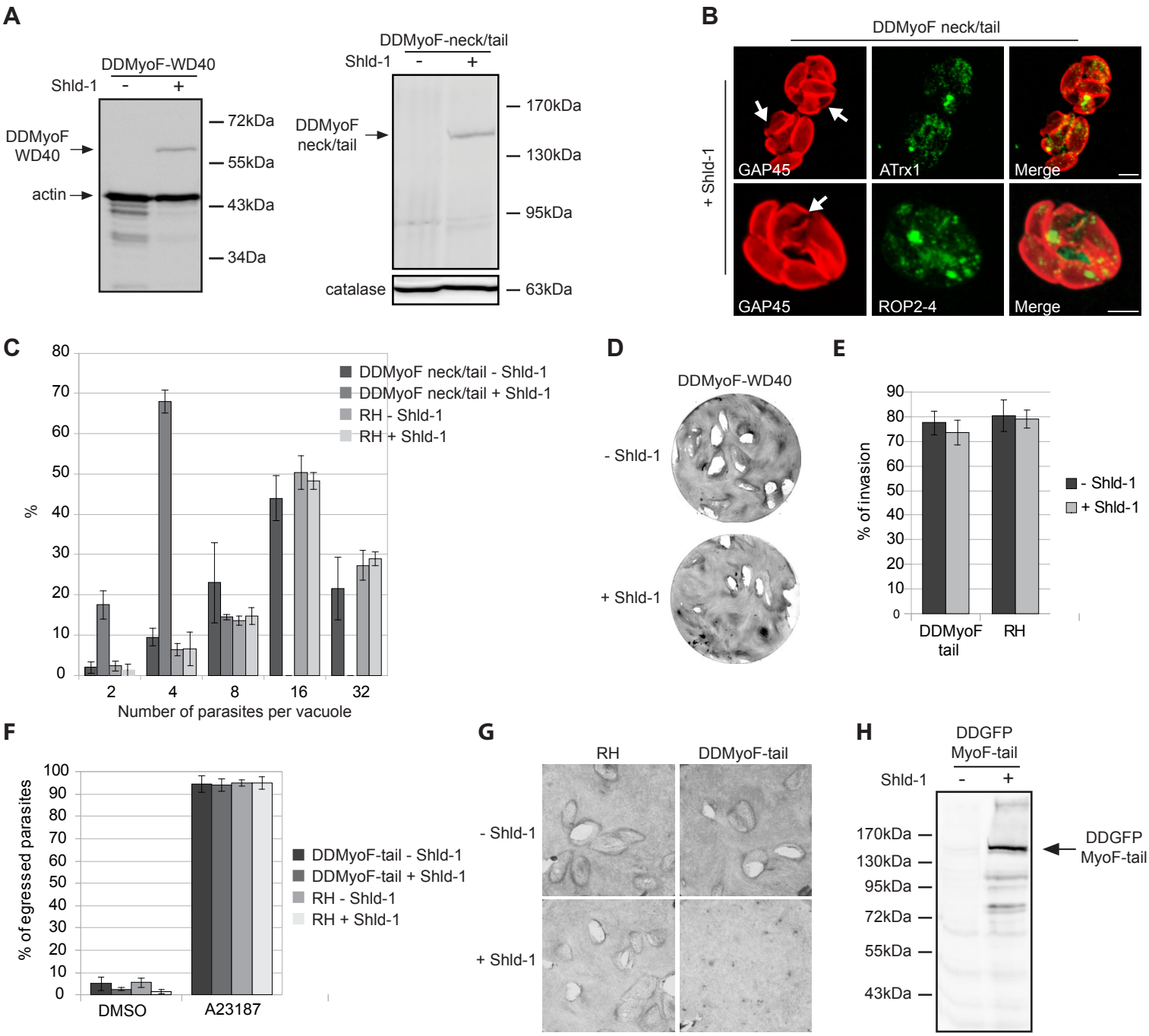
A
DDMyoF-WD40
Shld-1 - +
DDMyoF WD40
actin
72kDa
55kDa
43kDa
34Da
DDMyoF-neck/tail
Shld-1 - +
DDMyoF neck/tail
170kDa
130kDa
95kDa
catalase
63kDa
B
DDMyoF neck/tail
+ Shld-1
GAP45
ATrx1
Merge
GAP45
ROP2-4
Merge
C
% 80 70 60 50 40 30 20 10 0
DDMyoF neck/tail - Shld-1
DDMyoF neck/tail + Shld-1
RH - Shld-1
RH + Shld-1
2 4 8 16 32
Number of parasites per vacuole
D
DDMyoF-WD40
- Shld-1
+ Shld-1
E
% of invasion 90 80 70 60 50 40 30 20 10 0
- Shld-1
+ Shld-1
DDMyoF tail
RH
F
% of egressed parasites 100 90 80 70 60 50 40 30 20 10 0
DDMyoF-tail - Shld-1
DDMyoF-tail + Shld-1
RH - Shld-1
RH + Shld-1
DMSO
A23187
G
RH
DDMyoF-tail
- Shld-1
+ Shld-1
H
DDGFP MyoF-tail
Shld-1 - +
170kDa
130kDa
95kDa
72kDa
55kDa
43kDa
DDGFP MyoF-tail

Supplementary Movies Legends

Movie S1. DDMyoF-tail - Shld-1; Red, ACP-DsRed; Green, GFP-GAP45Ct. During division, daughter cell extension results in the formation of a U-shaped apicoplast which then undergoes fission and partitions between the two newly formed parasites.

Movie S2. DDMyoF-tail + Shld-1; Red, ACP-DsRed; Green, GFP-GAP45Ct. In both parasites, daughter cell tips appear on opposite sides of the mother cell. The apicoplast only associates with one daughter cell but fails to be incorporated. At the end of the division, the plastid is found in the basal end and is then deposited in the residual body.

Movie S3. DDMyoF-tail + Shld-1; Red, ACP-DsRed; Green, GFP-GAP45Ct. Left parasite: the apicoplast is properly localized between the two daughter cells but fails to remain associated during extension and is lost. Right parasite: daughter cells appear on opposite sides of the nucleus and the apicoplast fails to be incorporated. Following division, the apicoplast is found in the residual body.

Movie S4. DDMyoF-tail + Shld-1; Red, ACP-DsRed; Green, GFP-GAP45Ct. Daughter cells developed in opposite directions and the apicoplast failed to be incorporated.

Supplementary References

Agrawal S, van Dooren GG, Beatty WL, Striepen B (2009) Genetic evidence that an endosymbiont-derived endoplasmic reticulum-associated protein degradation (ERAD) system functions in import of apicoplast proteins. *J Biol Chem* **284:** 33683-33691

Beck JR, Rodriguez-Fernandez IA, Cruz de Leon J, Huynh MH, Carruthers VB, Morrissette NS, Bradley PJ (2010) A novel family of *Toxoplasma* IMC proteins displays a hierarchical organization and functions in coordinating parasite division. *PLoS Pathog* **6:** e1001094

Daher W, Plattner F, Carlier MF, Soldati-Favre D (2010) Concerted action of two formins in gliding motility and host cell invasion by *Toxoplasma gondii*. *PLoS Pathog* **6:** e1001132

DeRocher AE, Coppens I, Karnataki A, Gilbert LA, Rome ME, Feagin JE, Bradley PJ, Parsons M (2008) A thioredoxin family protein of the apicoplast periphery identifies abundant candidate transport vesicles in *Toxoplasma gondii*. *Eukaryot Cell* **7:** 1518-1529

Ding M, Clayton C, Soldati D (2000) Toxoplasma gondii catalase: are there peroxisomes in toxoplasma? *J Cell Sci* **113:** 2409-2419

El Hajj H, Papoin J, Cerede O, Garcia-Reguet N, Soete M, Dubremetz JF, Lebrun M (2008) Molecular signals in the trafficking of *Toxoplasma gondii* protein MIC3 to the micronemes. *Eukaryot Cell* **7:** 1019-1028

Frenal K, Polonais V, Marq JB, Stratmann R, Limenitakis J, Soldati-Favre D (2010) Functional dissection of the apicomplexan glideosome molecular architecture. *Cell Host Microbe* **8:** 343-357

Friedrich N, Santos JM, Liu Y, Palma AS, Leon E, Saouros S, Kiso M, Blackman MJ, Matthews S, Feizi T, Soldati-Favre D (2010) Members of a novel protein family containing microneme adhesive repeat domains act as sialic acid-binding lectins during host cell invasion by apicomplexan parasites. *J Biol Chem* **285:** 2064-2076

Herm-Gotz A, Weiss S, Stratmann R, Fujita-Becker S, Ruff C, Meyhofer E, Soldati T, Manstein DJ, Geeves MA, Soldati D (2002) *Toxoplasma gondii* myosin A and its light chain: a fast, single-headed, plus-end-directed motor. *EMBO J* **21:** 2149-2158

Pelletier L, Stern CA, Pypaert M, Sheff D, Ngo HM, Roper N, He CY, Hu K, Toomre D, Coppens I, Roos DS, Joiner KA, Warren G (2002) Golgi biogenesis in *Toxoplasma gondii*. *Nature* **418:** 548-552

Pino P, Aeby E, Foth BJ, Sheiner L, Soldati T, Schneider A, Soldati-Favre D (2010) Mitochondrial translation in absence of local tRNA aminoacylation and methionyl tRNA Met formylation in Apicomplexa. *Mol Microbiol* **76:** 706-718

Pino P, Foth BJ, Kwok LY, Sheiner L, Schepers R, Soldati T, Soldati-Favre D (2007) Dual targeting of antioxidant and metabolic enzymes to the mitochondrion and the apicoplast of *Toxoplasma gondii*. *PLoS Pathog* **3:** e115

Plattner F, Yarovinsky F, Romero S, Didry D, Carlier MF, Sher A, Soldati-Favre D (2008) *Toxoplasma* profilin is essential for host cell invasion and TLR11-dependent induction of an interleukin-12 response. *Cell Host Microbe* **3:** 77-87

Sadak A, Taghy Z, Fortier B, Dubremetz JF (1988) Characterization of a family of rhoptry proteins of *Toxoplasma gondii*. *Mol Biochem Parasitol* **29:** 203-211

Santos JM, Ferguson DJ, Blackman MJ, Soldati-Favre D (2011) Intramembrane cleavage of AMA1 triggers *Toxoplasma* to switch from an invasive to a replicative mode. *Science* **331:** 473-477

Wetzel DM, Hakansson S, Hu K, Roos D, Sibley LD (2003) Actin filament polymerization regulates gliding motility by apicomplexan parasites. *Mol Biol Cell* **14:** 396-406